IX CONGRESSO BRASILEIRO DE ENGENHARIA E CIÊNCIAS TÉRMICAS
9th BRAZILIAN CONGRESS OF THERMAL ENGINEERING AND SCIENCES

Paper CIT02-0288

GRAPHICAL DERIVATION OF THE EFFICIENCY OF AN ENDOREVERSIBLE CARNOT ENGINE AT MAXIMUM POWER OUTPUT

José Fiuza Branco
Dep. de Engenharia Mecânica e Gestão Industrial, Instituto Politécnico de Viseu, Campus Politécnico, 3504-510 VISEU, Portugal
jfiuza@demgi.estv.ipv.pt

Carlos Pinho
CEFT-DEMEGI, Universidade do Porto, Rua Dr. Roberto Frias, 4200-465 PORTO, Portugal
ctp@fe.up.pt

Rui de Almeida Figueiredo
Departamento de Engenharia Mecânica, Universidade de Coimbra, Pinhal de Marrocos, 3030-000 COIMBRA, Portugal
rui.figueiredo@mail.dem.uc.pt

Abstract. *The usefulness of the graphical representation of the thermodynamical laws is widely recognized. In this paper the Bejan-Bucher diagram is used in conjunction with a new graphical technique, which allows the deduction of the efficiency of an endo-reversible Carnot engine at maximum power conditions, using simple geometrical considerations. The present approach, unlike others available in the literature, may be directly applied to a Curzon-Ahlborn engine with different thermal resistances connecting to its thermal reservoirs.*

Keywords*. Bejan-Bucher diagram, Thermodynamics laws, endoreversible engines, graphical techniques, thermal efficiency.*

1. Introduction

In the past quarter of century, since the publication of the memorable paper of Curzon and Ahlborn (1975), the interest in the subject of endoreversible thermodynamics have been continuously growing; Hoffmann et al. (1997) have made a thorough review of the subject, presenting 170 references from both physicists and engineers. As an example of this interest tools have been developed that allow the graphical representation of the obtained results, namely of the so-called Curzon-Ahlborn efficiency.

In a reversible Carnot engine the heat exchanges between the working fluid and the cold and hot thermal reservoirs take place without any temperature difference; consequently they are infinitely slow. In the case of an endoreversible engine it is supposed that the internal reversibility exists, but the heat exchanges take place across a finite temperature difference, and across a finite thermal resistance, between the heat reservoirs and the working fluid.

The Novikov model of an endoreversible engine (model I) only considers a finite thermal resistance between the working fluid and the high temperature reservoir. The Curzon-Ahlborn model considers thermal resistances in both connections with the high and low temperature reservoirs. In the simpler case these thermal resistances may be assumed equal (model II), but in the more complex one (model III) they are different. For these kind of engines the thermal efficiency at maximum power conditions is usually known as the Curzon-Ahlborn efficiency; however, according to Bejan (1994), this result was previously derived by Novikov (1957) when analyzing the performance of nuclear power plants. Again in the context of nuclear power engineering, Chambadal (1957) arrived to this result considering a reversible engine receiving heat from a variable temperature hot stream, through a heat exchanger with an infinite heat-transfer area. El-Wakil (1962) also reported these results.

In all these cases, the performance of the power plant at maximum power output conditions is represented by

$$\eta_{CA} = 1 - \sqrt{\frac{TL}{TH}} \tag{1}$$

where TH and TL are the maximum and minimum temperatures of the available heat reservoirs and η_{CA} is the Curzon-Ahlborn efficiency, also known as the Curzon-Ahlborn-Novikov efficiency and Novikov-Chambadal-Curzon-Ahlborn efficiency. But it was with the paper of Curzon and Ahlborn that began an increasing interest in endoreversible thermal devices: engines, refrigerators and heat pumps, solar thermal and photo-voltaic engines, chemical engines, absorption refrigerators and in staged and combined systems (cf. Hoffmann at al., 1997; Boji□, 1997; Sun et al. 1997; Sahin and Kodal, 1999; Kodal et al., 2000; Chen et al., 2001; Zheng et al., 2002). For their results Novikov, Chambadal, Curzon and Ahlborn have been recognized by some as the founders of Finite Time Thermodynamics (cf. Denton, 2002).

Graphical derivations of the Curzon-Ahlborn results may be obtained using the Bejan-Bucher diagram, as stated by Yan and Chen (1990, 1992) and, more recently, by Chen and Andresen (1999). These authors considered models I and II. They assume that the developed graphical technique could be extended to model III using the concept of an equivalent temperature (Yan and Chen, 1992), but they do not present the corresponding modified diagram. Using a slightly modified Bejan-Bucher diagram, described in section 2, this paper presents a different diagrammatic construction that, using simple geometrical principles described in section 3, allows the graphical derivation of the Curzon-Ahlborn results for all the three above-referred models and of the thermodymamical laws describing this kind of engines. It is shown that the proposed formulation allows a straightforward extension to model III engines.

2. The Bejan-Bucher diagram

A diagram allowing the graphical representation of the first and second law of Thermodynamics for the case of reversible and irreversible engines was presented by Bejan (1977, 1982). Later it was introduced independently by Bucher (1986), for the case of the reversible Carnot engine and Wallingford (1989) extended the use of the Bucher diagram to the case of irreversible engines. The Bejan-Bucher diagram may also be used to represent the operation of refrigerators and heat pumps (Bejan 1977, 1982; Wallingford, 1989) and other type of reversible and irreversible thermodynamical processes (Bucher, 1993). According to Bejan (1996b), who refers it as the temperature-energy interaction (T-E) diagram, it was previously introduced in the Russian literature by Brodianskii (1973). Chen and Andresen (1999) point out that the diagram should be referred as Bejan diagram.

An example of the use of the diagram, for the case of a thermal engine, may be found in Fig. (1). The vertical line corresponds to the temperature scale and values corresponding to T=0, T=TH and T=TL are marked; the temperatures of the high-temperature reservoir and of the low-temperature one are TH and TL, respectively. A thermal engine operating between TH and TL, receives a given heat flow QH from the high-temperature reservoir, rejects QL to the low-temperature reservoir while producing work W.

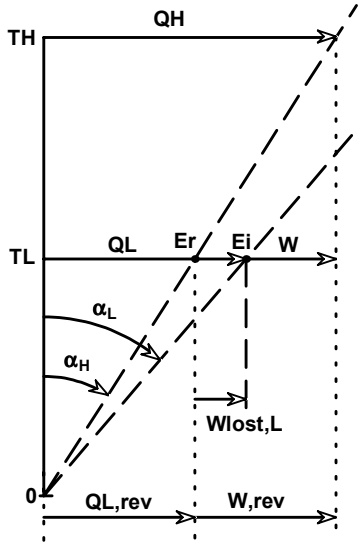

Figure 1. The Bejan-Bucher diagram illustrates energy conservation and entropy generation in a heat engine.

Figure 1 represents a reversible engine, 'Er', and an irreversible one, 'Ei'. Conservation of energy is illustrated simply by adding the arrows representing the energy fluxes. Entropy generation, S_{gen}, can be represented by the difference $\tan(\alpha_L)$–$\tan(\alpha_H)$; in the case of the reversible engine the entropy generation is zero. The lost of available work, according to the Gouy-Stodola theorem, is directly proportional to S_{gen} and to the reference temperature. This is also shown in Fig. 1: the lost of available work, represented at temperature TL, increases with the temperature.

3. A simple geometrical argument

In the present approach, it will be shown that the maximization of the power output of an endoreversible engine corresponds to the maximization of a rectangular area in the Bejan-Bucher diagram; more precisely it corresponds to the maximization of a rectangle inscribed in a triangle. This can be achieved finding another inscribed rectangle with the same area, as illustrated in Fig. 2.

The dimensions of rectangles $R1^r$ and $R2^r$, which have the same area, are related through: $L2^r = L^r - L1^r$ and $h2 = h - h1$. Similar relations may be written for the case of rectangles $R1^l$ and $R2^l$ and also for R1 and R2, where $R1 = R1^r + R1^l$ and $R2 = R2^r + R2^l$. Setting $h1 = h2$, or $L1^r = L2^r$ immediately leads to a rectangle with maximum area.

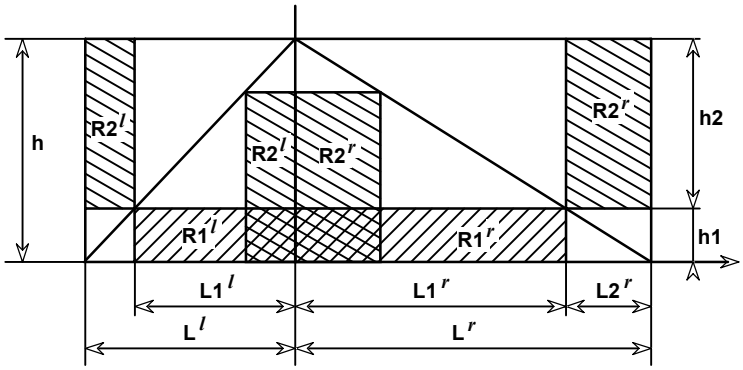

Figure 2. Illustration of the method used to obtain different inscribed rectangles with the same area.

4. Using the Bejan-Bucher diagram to derive the Curzon-Ahlborn efficiency: a new approach

An endoreversible Carnot engine is considered to be internally reversible. The existing irreversibilities are only external: associated with the heat exchange from the high-temperature reservoir, across a finite thermal resistance R_H, to the high-end temperature of the engine TH_E, and from the low-end temperature of the engine, TL_E, to the low-temperature reservoir, through the thermal resistance R_L. Temperatures of the thermal reservoirs are TH and TL as in Fig. 3, a simple scheme adapted from Chen and Andresen (1999).

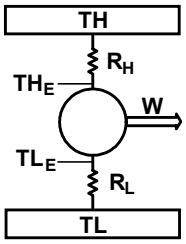

Figure 3. Schematic diagram of the Curzon-Ahlborn model of an endoreversible Carnot engine, from Chen and Andresen (1999).

The heat exchanges, which are considered to obey to the Newton law, may be written as

$$QH = (TH - TH_E)/R_H\,,\ QL = (TL_E - TL)/R_L \tag{2}$$

and applying the first and second laws of Thermodynamics to the Carnot engine, the following relations are obtained,

$$W = \eta QH,\quad \eta = (1 - TL_E/TH_E)\,,\ QH/TH_E = QL/TL_E \tag{3}$$

In the following development the three above-mentioned cases will be considered: model I ($R_H \neq 0$, $R_L = 0$), model II ($R_H = R_L \neq 0$) and model III ($R_H \neq R_L \neq 0$). In order to simplify the graphical representation, the Newton law may be written in a slightly different form

$$Q = \Ä T/R,\ \Rightarrow Q' = Q \times R = \Ä T \tag{4}$$

where Q' has dimensions of temperature and the thermal resistance R, used as a scaling variable, will be defined later for each of the three above referred cases; with this artifice Q'max=TH–TL is an evident maximum for Q', simplifying the implementation of the diagram. Branco et al. (2002) proposed a new thermodynamical diagram based on a further development of a similar approach.

4.1. The Novikov model ($R_H \neq 0$, $R_L = 0$)

In the case of the Novikov model the more evident choice for the scaling variable is $R = R_H$. If $TH_E = TH$ then QH=0 and consequently the power output is zero; in the other limit, when $TH_E = TL$ then QH is maximum but, from Eq. (3), the

power output is again zero. Somewhere between these limits there is a value of TH_E, which maximizes W. It can be graphically found using a slightly modified Bejan-Bucher diagram (Fig. 4a). To improve readability the same labels were used on the vertical left and right axis. Labels on the left axis are identified with the superscript '*l*' whereas labels on the right one are signalized with the superscript '*r*'. In the vertical axis temperatures T=0, T=TL and T=TH are marked and horizontal lines passing through each of these points are drawn. The horizontal axis represents values of Q', and from the choice of the scaling variable R, the line representing Eq. (4), line 'TH^l-TL^r', has an inclination of 45º. The right vertical axis passes through 'TL^r', and points '0' and 'TH^r' are also marked. At an arbitrary temperature TH_A point 'A' is marked on the diagram on the intersection of the line defining TH_A with the line defining the heat transfer law. At this temperature QH' corresponds to the segment 'TH_A^l-A'. The construction proceeds in the usual way: the reversible Carnot engine is represented by line 'A-0', which intersects TL at point 'B'; vertical auxiliary lines passing through points 'A' and 'B' are also drawn and points 'C', 'D', 'E' and 'F' defined. As in the non-modified Bejan-Bucher diagram segments 'TL^l-B' and 'B-F' represent the heat flow rejected at TL and the work delivery; but, in the present case and according to Eq. (4), these segments correspond to QL' and W'. Since the segment 'B-F' represents W' the hatched area [B,D,E,F] represents the product TL×W', and the maximization of W' may be achieved by maximizing this area.

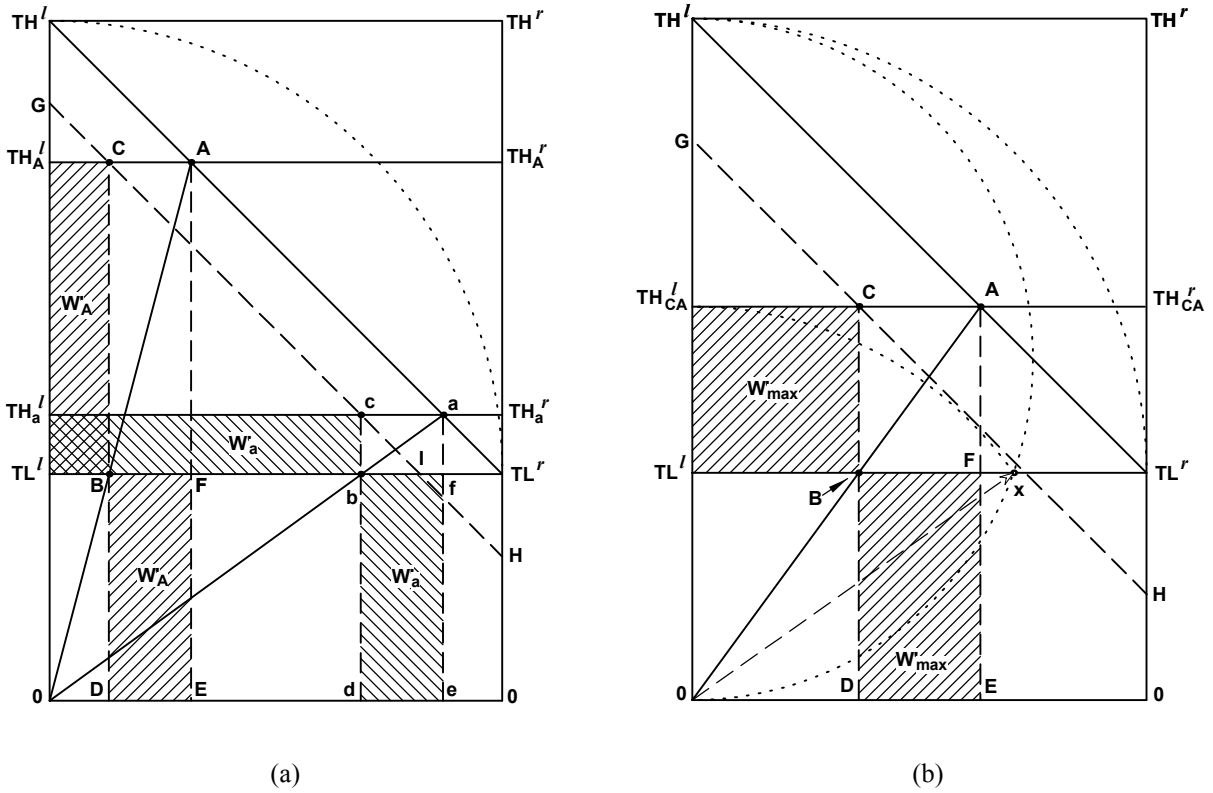

Figure 4. Diagram representing the Novikov engine (model I): (a) geometrical construction used to derive the performance at maximum output; (b) optimized engine for the same conditions used in (a).

From the observation of the diagram it is evident that the hatched rectangles [B,D,E,F] and [TL^l,B,C,TH_A^l] have the same area; its maximization is relatively simple. Line 'G-H', parallel to the line representing the heat transfer law, is drawn through 'C'; now the maximization problem is the maximization of rectangle [TL^l,B,C,TH_A^l], inscribed in triangle [TL^l,I,G]. According to the geometrical results referred in section 3, the high-end temperature TH_a of another engine producing the same work can be easily marked on the diagram. The relation between TH_a and TH_A can be expressed mathematically as

$$\overline{TH_A^l, G} = \overline{TL^l, TH_a^l} \tag{5}$$

where

$$\overline{TH_A^l, G} = \overline{TH_A^l, C} = \overline{TL^l, B} \text{ and } \overline{TL^l, TH_a^l} = TH_a - TL \tag{6}$$

On the other hand, considering similarity of triangles [0, A, TH_A^l] and [0, B, TL^l] and applying the Thales theorem results in the following equation

$$\frac{\overline{TL^l,B}}{\overline{0,TL^l}}=\frac{\overline{TH_A^l,A}}{\overline{0,TH_A^l}} \quad \Leftrightarrow \quad \overline{TL^l,B}=\frac{TL}{TH_A}\overline{TH_A^l,A} \quad \Leftrightarrow \quad \overline{TL^l,B}=\frac{TL}{TH_A}(TH-TH_A) \tag{7}$$

and combining Eqs. (5-7) leads to

$$TH_a-TL=\frac{TL}{TH_A}(TH-TH_A) \tag{8}$$

The rectangle of maximum area is obtained when $TH_A=TH_a=TH_{CA}$, hence

$$TH_{CA}=\sqrt{TL\times TH} \tag{9}$$

and the efficiency of the Novikov engine may be immediately found. The obtained result is, as expected, the Curzon-Ahlborn efficiency

$$\eta_{CA}=1-\frac{TL}{TH_{CA}}=1-\sqrt{\frac{TL}{TH}} \tag{10}$$

Figure (4b) shows the geometrical construction used to represent the diagram corresponding to the Novikov engine with maximum power output; the key point is the consideration that segment '0-x' represents $(TL\times TH)^{1/2}$: point 'x' is obtained intersecting a circumference with diameter '0-TH^l' and the line 'TL^l-TL^r' (Henderson, 1996). An arc with center in '0' and radius '0-x' defines the optimum temperature $TH_{E,opt}=TH_{CA}$.

4.2. The Curzon-Ahlborn model with $R_H=R_L\neq 0$

In the case of the Curzon-Ahlborn model with equal high and low end resistances (Curzon and Ahlborn, 1975; Rubin, 1979), the sum of these resistances, $R=R_H+R_L$ may be used as the scaling variable; with this choice the maximum heat flow from/to the thermal reservoirs will be QH'max=QL'max=2(TH–TL). As a result the heat transfer laws are represented by lines with slopes ±1/2.

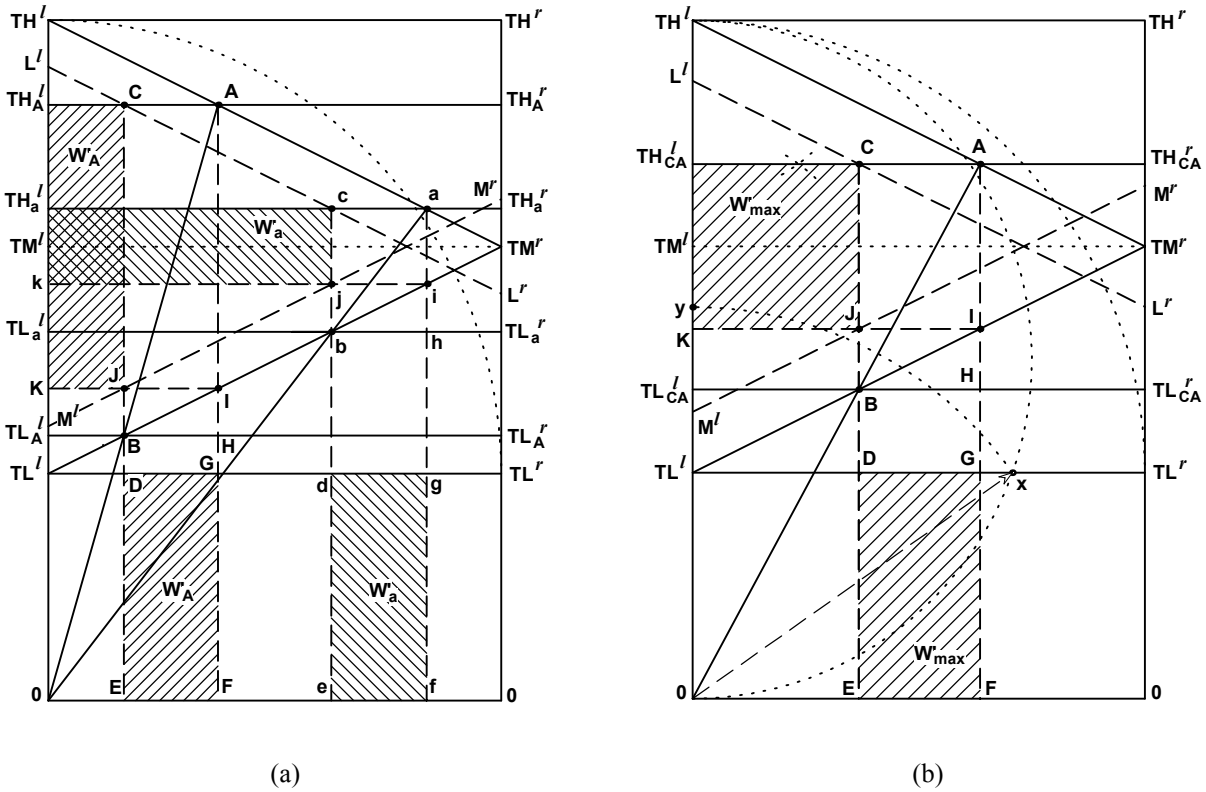

(a) (b)

Figure 5. Diagram representing the Curzon-Ahlborn engine (model II): (a) geometrical construction used to derive the performance at maximum output; (b) optimized engine for the same conditions used in (a).

In the diagram of Fig. (5a) temperatures T=0, TL and TH are marked in the right vertical axis and, at a distance equal to (TH–TL), a second vertical axis is drawn. Temperature TM=1/2(TL+TH) is also marked in the diagram; the heat transfer laws are lines 'TH^{l}-TM^{r}' and 'TL^{l}-TM^{r}'. A high-end temperature of the engine TH_A is arbitrarily chosen and point 'A' marked at the intersection with line 'TH^{l}-TM^{r}'. The line 'A-0' represents the reversible part of the engine and point 'B', at the intersection with line 'TL^{l}-TM^{r}', defines the low-end temperature TL_A. Auxiliary vertical lines passing through points 'A' and 'B' define points 'C' through 'I', and a horizontal line passing through point 'I' defines points 'J' and 'K'. Segments 'TL_A^{l}-B' and 'B-H' represent the heat rejected to the low temperature reservoir and the delivered work. Auxiliary slanted lines passing through points 'C' and 'J' and parallel to 'TH^{l}-TM^{r}' and 'TL^{l}-TM^{r}' are also drawn.

As before, the maximization of the work may be achieved maximizing the product W'×TL represented by the rectangle [D,E,F,G] area, which equals the rectangle [J,C,TH_A^{l},K] area. As in section 4.1 the high-end temperature TH_a of another engine delivering the same power must verify the following condition

$$\overline{\mathrm{TH}_{\mathrm{A}}^{l},\mathrm{L}^{l}} = \overline{\mathrm{TM}^{l},\mathrm{TH}_{\mathrm{a}}^{l}} \tag{11}$$

Considering the slope of line 'L^{l}-L^{r}' and the definition of TM, the above equation may be written as

$$\overline{\mathrm{TH}_{\mathrm{A}}^{l},\mathrm{L}^{l}} = \overline{\mathrm{TM}^{l},\mathrm{TH}_{\mathrm{a}}^{l}} \quad \Leftrightarrow \quad \frac{\overline{\mathrm{TL}_{\mathrm{A}}^{l},\mathrm{B}}}{2} = \mathrm{TH}_{\mathrm{a}} - \frac{\mathrm{TH}+\mathrm{TL}}{2} \tag{12}$$

On the other hand, applying the Thales theorem to triangle [0,A,TH_A^{l}], while bearing in mind that the slope of lines 'L^{l}-L^{r}' and 'M^{l}-M^{r}' is ±1/2, leads to the equation

$$\frac{\overline{\mathrm{TH}_{\mathrm{A}}^{l},\mathrm{A}}}{\overline{0,\mathrm{TH}_{\mathrm{A}}^{l}}} = \frac{\overline{\mathrm{TL}_{\mathrm{A}}^{l},\mathrm{B}}}{\overline{0,\mathrm{TL}_{\mathrm{A}}^{l}}} \quad \Leftrightarrow \quad \frac{2(\mathrm{TH}-\mathrm{TH}_{\mathrm{A}})}{\mathrm{TH}_{\mathrm{A}}} = \frac{2(\mathrm{TL}_{\mathrm{A}}-\mathrm{TL})}{\mathrm{TL}_{\mathrm{A}}} \quad \Leftrightarrow \quad \mathrm{TL}_{\mathrm{A}} = \frac{\mathrm{TL}\times\mathrm{TH}_{\mathrm{A}}}{2\mathrm{TH}_{\mathrm{A}}-\mathrm{TH}} \tag{13}$$

which may be combined with Eq. (12) to obtain

$$\frac{\overline{\mathrm{TL}_{\mathrm{A}}^{l},\mathrm{B}}}{2} = \mathrm{TL}_{\mathrm{A}} - \mathrm{TL} = \mathrm{TH}_{\mathrm{a}} - \frac{\mathrm{TH}+\mathrm{TL}}{2} \quad \Leftrightarrow \quad \frac{\mathrm{TL}\times\mathrm{TH}_{\mathrm{A}}}{2\mathrm{TH}_{\mathrm{A}}-\mathrm{TH}} - \mathrm{TL} = \mathrm{TH}_{\mathrm{a}} - \frac{\mathrm{TH}+\mathrm{TL}}{2} \tag{14}$$

When TH_a=TH_A the product W'×TL is maximum; hence the optimum temperature, $TH_{E,opt}$=TH_{CA}, is

$$\mathrm{TH}_{\mathrm{CA}} = \frac{\mathrm{TH}+\sqrt{\mathrm{TL}\times\mathrm{TH}}}{2} \tag{15}$$

and the thermal efficiency of the engine is

$$\eta_{\mathrm{CA}} = 1 - \frac{\mathrm{TL}_{\mathrm{CA}}}{\mathrm{TH}_{\mathrm{CA}}} = 1 - \frac{\mathrm{TL}}{2\mathrm{TH}_{\mathrm{CA}}-\mathrm{TH}} = 1 - \sqrt{\frac{\mathrm{TL}}{\mathrm{TH}}} \tag{16}$$

The engine delivering maximum power is represented in the diagram of Fig. (5b), where TH_{CA} is marked right in the middle of the segment 'y-TH^{l}'; the length of segment '0-y' is $(TL\times TH)^{1/2}$, and was drawn through the same geometrical construction used in Fig. (4b).

4.3. The Curzon-Ahlborn model with $R_H \neq R_L \neq 0$

As mentioned in the introduction, the graphical representation of endoreversible engines at maximum power output, in the conditions described in the two previous subsections, has been accomplished by other authors, namely Chen and Andresen (1999). According to these authors the case of different thermal resistances could be treated introducing the concept of equivalent temperature, defined by Yan and Chen (1992). With the present approach there is a straight-forward extension to this more complex case. As before, the scaling variable is the sum of the thermal resistances R, the individual resistances being expressed as $R_H=\phi R$ and $R_L=(1-\phi)R$ (cf. Bejan, 1996b). The heat flows to and from the Carnot engine are

$$\mathrm{QH}' = \frac{\mathrm{TH}-\mathrm{T}}{\ddot{\mathrm{o}}}, \quad \mathrm{QL}' = \frac{\mathrm{T}-\mathrm{TL}}{1-\ddot{\mathrm{o}}} \tag{17}$$

and when QH'=QL'=TH–TL, both equations lead to T=TM=TH–ϕ(TH–TL). In the corresponding diagram, Fig. (6a), lines representing the heat flows have slopes –ϕ, line 'TH^l-TM^r', and (1–ϕ), line 'TL^l-TM^r'. From the choice of TH_A the construction of the diagram follows the same rules presented in section 4.2. TH_a, the high-end temperature of an engine delivering the same power, is also represented in the diagram and, according to the result of section 3, TH_a relates with TH_A through

$$\overline{TH_A^l, L^l} = \overline{TM^l, TH_a^l} \tag{18}$$

Considering the slope of lines 'TH^l-TM^r' and 'TL^l-TM^r' Eq. (18) takes the following form

$$\overline{TH_A^l, L^l} = \phi \times \overline{TH_A^l, C} = \phi \times \overline{TL_A^l, B} = \frac{\phi}{1-\phi}(TL_A - TL) = TH_a - TH + \phi(TH - TL) \tag{19}$$

on the other hand, from the Thales theorem applied to triangle $[0,A,TH_A^l]$

$$\frac{\overline{TL_A^l, B}}{\overline{0, TL_A^l}} = \frac{\overline{TH_A^l, A}}{\overline{0, TH_A^l}} \quad \Leftrightarrow \quad \frac{(TL_A - TL)/(1-\phi)}{TL_A} = \frac{(TH - TH_A)/\phi}{TH_A} \quad \Leftrightarrow \quad TL_A = \frac{\phi TL \times TH_A}{TH_A - (1-\phi)TH} \tag{20}$$

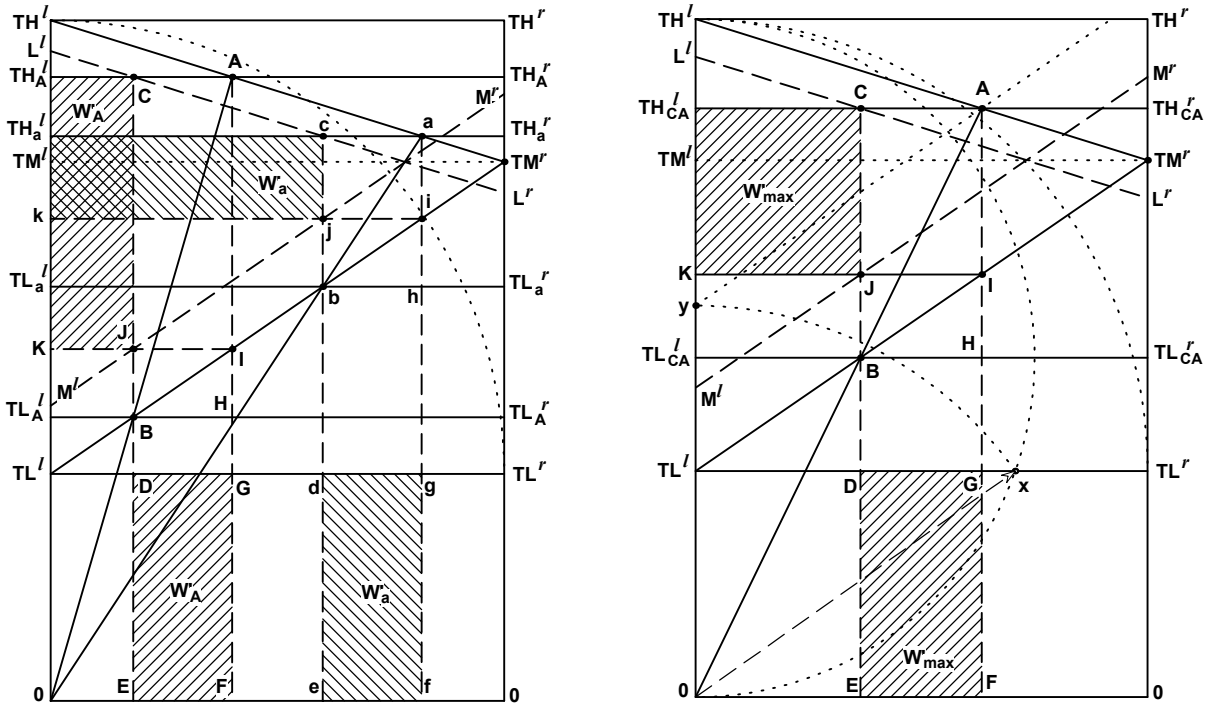

(a) (b)

Figure 6. Diagram representing the Curzon-Ahlborn engine (model III): (a) geometrical construction used to derive the performance at maximum output; (b) optimized engine for the same conditions used in (a).

Combining these two equations at maximum output conditions (TH_a=TH_A=TH_{CA}) results in

$$TH_{CA} = (1-\phi)TH + \phi\sqrt{TL \times TH} \tag{21}$$

The corresponding thermal efficiency is again given by the Curzon-Ahlborn formula

$$\eta_{CA} = 1 - \frac{TL_{CA}}{TH_{CA}} = 1 - \frac{\phi TL}{TH_{CA} - (1-\phi)TH} = 1 - \sqrt{\frac{TL}{TH}} \tag{22}$$

and the power output is

$$W = \left(\sqrt{TH} - \sqrt{TL}\right)^2 / R \tag{23}$$

This result is a consequence of the choice of R as a scaling variable, as an attempt to simplify the graphical representation. Usually the heat flows are calculated using the concept of thermal conductance, defined as the product of an overall heat transfer coefficient and a contact area (UA). For each of the heat transfer processes the thermal resistance is the inverse of the thermal conductance. If a fixed total conductance UA and individual conductances defined as $UA_H = xUA$ and $UA_L = (1-x)UA$ were considered (Bejan, 1988, 1996b) the analysis would be somewhat different; nevertheless the following relations between R, UA, ϕ and x can be easily established

$$R^{-1} = x(1-x)UA; \quad x = 1 - \phi \tag{24}$$

and Eq. (23), written in terms of UA, takes the usual form

$$W = x(1-x)UA\left(\sqrt{TH} - \sqrt{TL}\right)^2 \tag{25}$$

Figure (6b) represents an engine working at maximum output conditions, for the same value of ϕ used in Fig. (6a). The temperature TH_{CA} corresponds to the intersection of the line defining the high-end heat transfer law with a parallel to the low-end one passing through point 'y'. The construction of the diagram follows the rules presented before.

5. Conclusions

Based on the use of a slightly modified Bejan-Bucher diagram, a procedure was presented that allows the performance at maximum output of an endoreversible Carnot engine to be derived through the use of simple geometrical principles. The Novikov and Curzon-Ahlborn models were treated. With the present approach the case of a Curzon-Ahlborn engine with different thermal resistances between the engine and the high and low temperature reservoirs was treated in a straightforward manner. In the modified diagram the second-law efficiency, availability loss and entropy generation could also be represented, as mentioned in section 2, as a direct extension of the results of Bejan (1982), Wallingford (1989) and Chen and Andresen (1999).

6. Acknowledgement

The first author gratefully acknowledges the support of PRODEP II (Programa de Desenvolvimento Educativo para Portugal).

7. References

Bejan, A., 1977, "Graphic Techniques for Teaching Engineering Thermodynamics, Mech. Eng. News, Vol.14, No. 2, pp. 26-28.

Bejan, A., 1982, "Entropy Generation Through Heat and Fluid Flow", Wiley, New York.

Bejan, A., 1988, "Theory of Heat Transfer-Irreversible Power Plants", Int. J. Heat Mass Transfer Vol.31, pp. 1211-1218.

Bejan, A., 1994, "Engineering Advances in Finite-Time Thermodynamics", Am. J. Phys. Vol.62, pp. 11-12.

Bejan, A., 1996a, "Models of Power Plants that Generate Minimum Entropy while Operating at Maximum Power", Am. J. Phys. Vol.64, pp. 1054-1059.

Bejan, A., 1996b, "Entropy Generation Minimization", CRC Press, Boca Raton.

Boji□, M., 1997, "Cogeneration of Power and Heat by Using Endoreversible Carnot Engine", Energy Convers. Mgmt., Vol.38, pp 1877-1880.

Branco, J. F., Pinho, C. T. and Figueiredo, R. A., 2002, "First and Second-Law Efficiencies in a New Thermodynamical Diagram", J. Non-Equilib. Thermodyn., accepted for publication.

Brodianskii, V. M., 1973, "Exergetic Method of Thermodynamic Analysis", Energia, Moscow.

Bucher, M., 1986, "New Diagram for Heat Flows and Work in a Carnot Cycle", Am. J. Phys. Vol.54, pp. 850-851.

Bucher, M., 1993, "Diagram of the Second Law of Thermodynamics", Am. J. Phys. Vol.61, pp. 462-466.

Chambadal, P., 1957, "Les Centrales Nucleaires", Armand Colin, Paris.

Chen, J. and Andresen, B., 1999, "Diagrammatic Representation of the Optimal Performance of an Endoreversible Carnot Engine at Maximum Power Output", Eur. J. Phys., Vol.20, pp. 21-28.

Chen, J., Yan, Z., Lin, G. and Andresen, B., 2001, "On the Curzon-Ahlborn Efficiency and its Connection with the Efficiencies of Real Heat Engines", Energy Convers. Mgmt., Vol.42, pp 173-181.

Curzon, F.L.and Ahlborn, B., 1975,"Efficiency of a Carnot Engine at Maximum Power Output", Am. J. Phys. Vol.43, pp. 22-24.

Denton, J. C., 2002, "Thermal Cycles in Classical Thermodynamics and Nonequilibrium Thermodynamics in Contrast with Finite Time Thermodynamics", Energy Convers. Mgmt., Vol.43, pp 1583-1617.

El-Wakil, M. M., 1962, “Nuclear Power Engineering”, McGraw-Hill, New York.

Henderson, D.W., 1996, “Experiencing Geometry: On Plane and Sphere”, Prentice Hall, New York.

Hoffmann, K. H., Burzler, J.M. and Schubert, S., 1997, “Endoreversible Thermodynamics”, J. Non-Equilib. Thermodyn., Vol.22, pp. 311-355.

Kodal, A., Sahin, B. and Yilmaz, T., 2000, “A Comparative Performance Analysis of Irreversible Carnot Heat Engines under Maximum Power Density and Maximum Power Conditions”, Energy Convers. Mgmt., Vol.41, pp 235-248.

Novikov, I. I., 1958, “The efficiency of Atomic Power Stations”, J. Nucl. Energy II, Vol. 7, pp 125-128, translated from Novikov, I. I., 1958, Atomnaya Energiya, Vol. 3 (11), p. 409.

Rubin, M. H., 1979, “Optimal Configuration of a Class of Irreversible Heat Engines. I’, Phys. Rev. A, Vol.19, pp 1272-1276.

Sahin, B. and Kodal, A., 1999, “Finite Time Thermoeconomic Optimization for Endoreversible Refrigerators and Heat Pumps”, Energy Convers. Mgmt., Vol.40, pp 951-960.

Sun, F., Chen, W., Chen L. and Wu, C., 1997, “Optimal Performance of an Endoreversible Carnot Heat Pump”, Energy Convers. Mgmt., Vol.38, pp 1439-1443.

Wallingford, J., 1989, “Inefficiency and Irreversibility in the Bucher Diagram”, Am. J. Phys. Vol.57, pp. 379-381.

Yan, Z.and Chen, J., 1990, “Modified Bucher Diagram for Heat Flows and Works in Two Class of Cycles”, Am. J. Phys. Vol.58, pp. 404-405.

Yan, Z.and Chen, J., 1992, “New Bucher Diagram for a Class of Irreversible Carnot Cycles”, Am. J. Phys. Vol.60, pp. 475-476.

Zhen, J. Chen, L. Sun, F. and Wu, C., 2002, “Powers and Efficiency Performance of an Endoreversible Braysson Cycle”, Int. J. Thermal Sci., Vol.41, pp. 201-205.